Note CELESTE: Observing proposal for the detection of neutralino annihilation photons from DRACO with CELESTE

Edmond Giraud[1], Julien Lavalle[1], Mariusz Sapinski[1], Javier Bussóns[1], Alain Falvard[1], Agnieszka Jacholkowska[1], Eric Nuss[1], and Frédéric Piron[1]

Groupe d'Astroparticules de Montpellier, Place Eugène Bataillon, CC85, 34095 Montpellier Cedex, France

Abstract. The objective of this project is to probe a fraction of the supersymmetric parameter space by assuming that the halo of the dwarf spheroidal (dSph) DRACO is made of neutralinos (χ). This satellite of the Galaxy has long been considered as a potential candidate for indirect search of dark matter [1] because of its huge mass-to-light ratio, $M/L > 200$, compared to that of bright spiral galaxies (~ 10). An important effort was made in 2000/1 both on the observational side [2] and on dynamical methods [3] in order to derive a mass density profile of this object based upon radial velocities of individual stars. The first clear signature of an extended dark matter halo came in November 2001 [4]. DRACO would be one of the numerous large clumps predicted by Cold Dark Matter (CDM) scenarios which would not be disrupted by the galactic tidal field [5], [6]; indeed the data indicate that DRACO has not been tidally truncated within $\sim 1kpc$ [4]. At a distance of 82 ± 7 kpc [7] and with a halo mass of $8^{+3}_{-2} \times 10^7$ $M_\odot$ [4], a fraction of neutralino models would be within the reach of CELESTE if an exceptional effort in observation is made.

1 The observational case for DRACO

1.1 The Draco dSph

Located at 82 ± 7 kpc [7], DRACO (UGC 10822) is one of the many Local Group dwarf spheroidal galaxies. It is a satellite of our own Galaxy, visible in the northern hemisphere at $\alpha = 17h20m12.39s$; $\delta = +57d54m55.3s$ (2000), i.e. in May-June from the Thémis-CELESTE Observatory. The DRACO dSph has a central stellar mass-to-light ratio of ~ 60 [7]. Being rather nearby and massive, this small galaxy was considered as a possible candidate for the detection of neutralino annihilation photons in early neutralino simulations [1], together with Carina, Ursa Minor and Sextans. Unlike disk dwarf spirals, which are gas rich systems, the stellar kinematics of gas-free dSph's is not dominated by a rotating disk but rather by quasi-isotropic orbits.

1.2 Stellar content

Out of 284 stars observed in 2000 by [2] in the DRACO region with a multi-fiber spectrograph mounted on the WH 4-m telescope, 159 turned out to be DRACO members with sufficiently good spectra to be included in a dynamical analysis [2]. The DRACO stellar population deduced from HST color-magnitude diagrams is intermediate-age to old, similar to halo globular clusters, with little spread in age and without significant star formation in the last ~ 5 Gyr [8]. As a consequence, the stars should be well-mixed so there is no need to use multi-component models (like multi-King or other).

1.3 Mass distribution

Until recently, dSph's were fitted using King models which require two strong assumptions: 1) the mass distribution follows the light distribution and 2) the stellar orbits are isotropic. Since the stars in a dSph are a tiny fraction of its mass, dynamical models have been developed to account for the case where the mass would not follow the stellar distribution [3]. With the present data and models, [4] showed the first clear evidence of an extended halo in DRACO (Fig. 1 from [4]). The velocity dispersion profile is flat or slowly rising at large radii and rotation is negligible. Unlike typical nearby globular clusters, the outermost regions of DRACO are strongly dark-matter-dominated. The mass-to-light ratio reaches a value > 200 and a mass of $8^{+3}_{-2} \times 10^7$ $M_\odot$ at 3 core radii (i.e. the mass does not follow the light). The tidal radius due to the Galactic gravitational field is several times the length scale of the luminous matter, so [4] argues against tidal forces having played a major role in the dynamical evolution of DRACO.

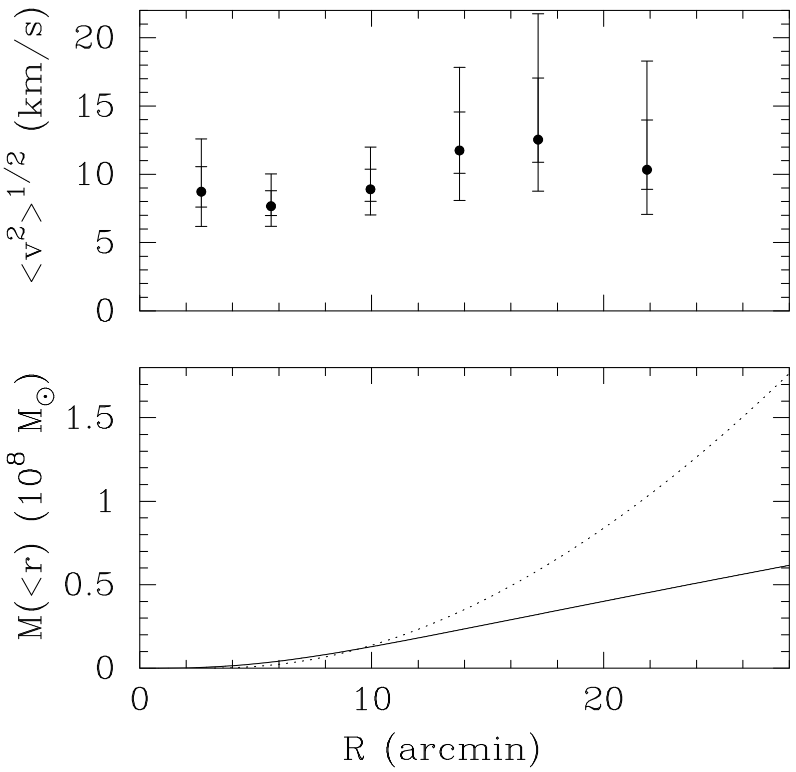

Fig. 1. Velocity profile of DRACO and 3-D mass profiles from Jeans equations (taken from [4]). Errorbars are for 1σ and 2σ. At 82 kpc, 1 arcmin = 0.024 kpc.

1.4 Central profile

As clearly indicated in [4], present data are not sufficient to discriminate strongly between cored and cuspy profiles for DRACO's dark halo so we have to rely on cosmological simulations which, as we see below, favour cuspy halos.

2 The theoretical case for DRACO

2.1 The CDM scenario

Most cosmological models studied today are variants of the CDM scenario, where perturbations start in a WIMP medium. Due to the small thermal velocity of CDM, fluctuations survive from the early universe on all scales. CDM is a bottom-up scenario whereby larger structures develop as small clumps collapse and undergo series of mergers resulting in the hierarchical formation of massive dark matter halos. These halos are the hosts of baryonic systems, from galaxies to clusters, which cooled down and condensed into more compact, bounded structures by dissipating energy. Cosmological N-body simulations describe well this non-linear, complex series of mergers, accretion events and violent relaxations which are in general agreement with observations but experience some problems on small scales [9], [10]. An overview of these issues was recently presented by [11]. A major point is that halos obtained by these hierarchical N-body simulations are cuspy on all scales, with inner profiles ranging between r^{-1} [12] to $r^{-1.5}$ [13].

2.2 Sub-halos are cuspy

The first simulations of the growth of CDM halos found smooth tri-axial structures, but higher resolution numerical simulations revealed that a significant fraction of the mass lies in substructures (sub-halos) orbiting in virialized dark matter halos [14], [15], [16]. DRACO would appear as one of the most massive substructure orbiting around the Galaxy. Substructures seem to extend down to the smallest mass scale, well below that of dSph's. Indeed the case of a DRACO-type object having a mass of 10^8 $M_\odot$ was studied at high resolution [6] with several millions particles. It turned out that, even on this small scale, the density profile of this mini-halo has a singular central cusp (Fig. 2 taken from [6]) and that the smooth halo is surrounded by a large amount of substructures.

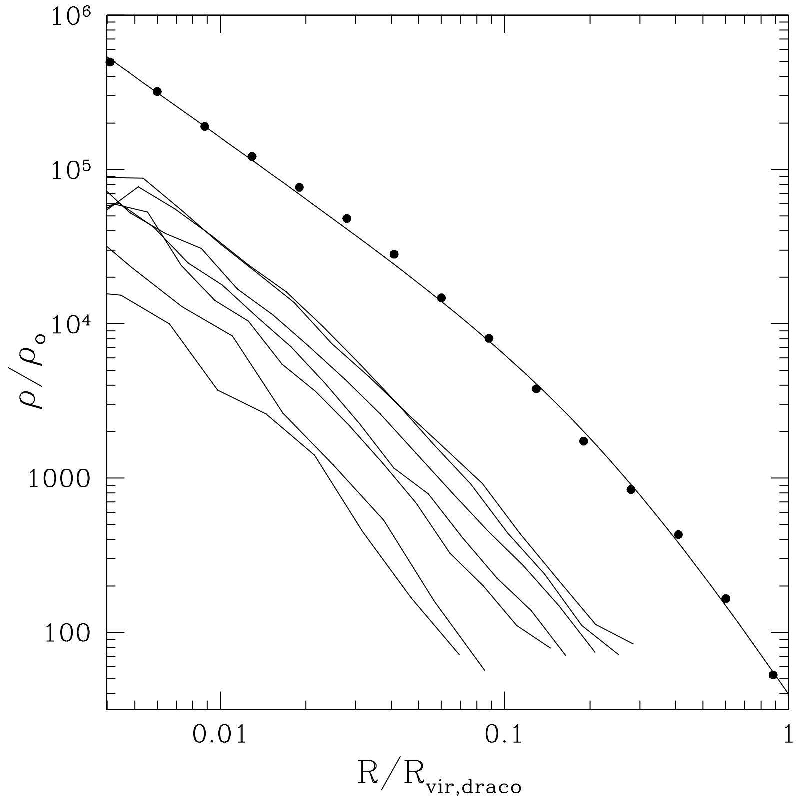

Fig. 2. Example of density enhancement profile of a "DRACO-type" mini-halo extracted from a snapshot at z = 4 of a CDM simulation started at z = 100. (from [6]). The inner slope goes as $r^{-1.3}$
.

It is interesting to note that fractal distributions are not a novelty in astrophysics: molecular clouds in the interstellar medium are known to have a fractal spatial distribution [20]. In order to explain the cored profiles found in gas-rich dwarves, it has been proposed that a fraction of dark matter may be in the form of cold, primordial fractal baryonic clouds (see [21] and references therein).

2.3 Some sub-halos survive

The number of substructures in a galaxy halo predicted by the CDM scenario is larger than the number of dwarf satellites and globular clusters observed in the Galaxy and in M31 [15], [17]. It is well-known, however, that globular clusters continuously loose stars due to tidal forces from the halo gravitational potential. Mass is stripped from the outer regions of globular clusters and evaporates mainly at each passage through the disk. This is why it is generally argued that globular clusters do not have dark matter except perhaps in an inner bubble. The structural evolution of sub-halos was recently analyzed in [5]. This paper gives the conditions under which Navarro-Frenk-White (NFW) sub-halos are fully disrupted and shows that the tidal radius of a dSph like DRACO is well beyond the optical radius. This may also explain why the distant globular cluster Palomar 13 (D = 24.3 kpc) is well fitted both by a King profile with a power-law tail and by a NFW profile [18], i.e. this globular cluster would be the first observed case of Galactic dark clump which has not been destroyed by the Galactic tidal field [19].

3 The DRACO halo profile

Since the velocity data do not sample the inner 2 arcmin, they cannot discriminate between cored and cuspy profiles. Both the NFW profile in r^{-1} and the Moore profile in $r^{-1.5}$ are able to fit the observed flat velocity profile. Indeed, as it was pointed out in [6], very similar bounding velocity profiles may be obtained by playing with the concentration parameter. This is illustrated in Fig. 3 for a "DRACO-type" simulated object.

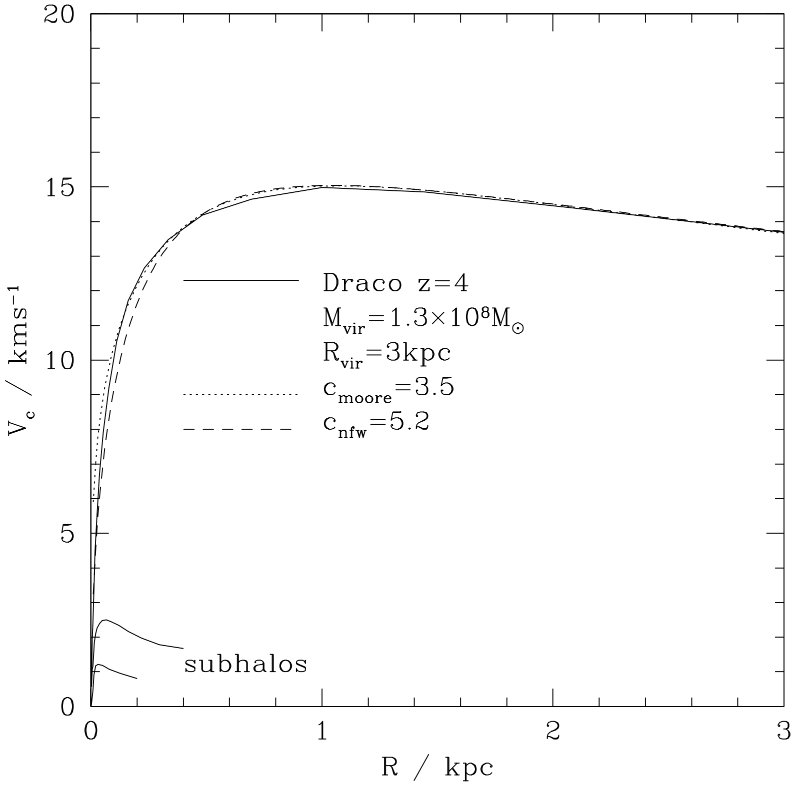

Fig. 3. Bounding velocity curve of a "DRACO-type" mini-halo at z = 4 from the same simulation as in Fig. 1 (solid curve), NFW profile (dashed curve) and Moore profile (dotted curve) (from [6]). Today the simulated mini-halo is more concentrated: c_{nfw} lies between 14 (no mass loss) and 11 (95% tidal mass loss) [5].

An r^{-2} profile was recently used to estimate the photon flux that would have been detected by EGRET if the DRACO halo were made of neutralinos [22]. With such a singular isothermal profile (SIS), the density blows up at the center and [22] indicates that most of the neutralino parameter space would have been explored by EGRET. A SIS profile does not seem to be forbidden by the data but there is no theoretical support for it and such a singularity has never been reported in CDM simulations. Therefore we do not consider this (extremely favourable) case. An NFW profile is given by:

$$\rho(r) = \rho_0 \frac{r_s}{r} \left(1 + \frac{r}{r_s}\right)^{-2}, \tag{1}$$

where the scale parameter r_s and the density ρ_0 are derived from the velocity profile through the equation:

$$M(R) = 4\pi \int_0^R \rho_0 \frac{r_s}{r} \left(1 + \frac{r}{r_s}\right)^{-2} r^2 dr, \tag{2}$$

which results in:

$$M(R) = 4\pi\rho_0 r_s^3 \left[ln(1 + R/r_s) + \frac{1}{1 + R/r_s} - 1\right]. \tag{3}$$

The bounding velocity is given by:

$$v^2(R) = 4\pi G\rho_0 \frac{r_s}{R}\left[ln(1+R/r_s) + \frac{1}{1+R/r_s} - 1\right] r_s^2. \tag{4}$$

Moore's profile is parametrized as:

$$\rho(r) = \rho_0 \left(\frac{r_c}{r}\right)^{1.5}\left(1+\frac{r}{r_c}\right)^{-1.5}, \tag{5}$$

which gives:

$$M(R) = 4\pi\rho_0 r_c^3\left[ln\left(1/2 + \frac{R}{r_c} + \sqrt{\frac{R}{r_c}\left(1+\frac{R}{r_c}\right)}\right) - ln(1/2) - 2\sqrt{\frac{\frac{R}{r_c}}{1+\frac{R}{r_c}}}\right], \tag{6}$$

and, therefore:

$$v^2(R) = 4\pi G\rho_0 \frac{r_c}{R}\left[ln\left(1/2 + \frac{R}{r_c} + \sqrt{\frac{R}{r_c}\left(1+\frac{R}{r_c}\right)}\right) - ln(1/2) - 2\sqrt{\frac{\frac{R}{r_c}}{1+\frac{R}{r_c}}}\right] r_c^2, \tag{7}$$

which we compare with the mass profile deduced from the data.

3.1 Mass models with one component

Figure 4 shows the velocity curve with 1 σ error bars and a best NFW fit obtained by adjusting the two free parameters ρ_0 and r_s. We have also obtained the best fits for the upper $v + 1\ \sigma$ (NFWu) and the lower $v - 1\ \sigma$ (NFWd) curves. As the data error bars are quite large, so are the differences between the NFWu and NFWd models. In addition to this, the inner and outer points of the velocity profile cannot be matched correctly by the type of distribution which we have forced through the data.

This type of velocity profile is reminiscent of two-component distributions with different scales as, for example, a galaxy system with a bulge and a disk (like the rotation curve of M31). Here there is no direct visual support for two components but one may think of a merging system resulting from a compact component and a larger halo, both originally with a similar CDM profile. These CDM sub-halos have merged and are presently seen at an epoch when the centers of mass are roughly at the same position but do not yet form either a single NFW or a Moore halo. This may seem like an ad-hoc tricky model but it is not more so than the M31 model. Another possibility is the presence of a central black hole. In the next paragraphs we shall consider both cases.

Table 1. Parameters of mass models with one or two components without Massive Black Hole (MBH).

model	ρ_0 ($10^{-24}\ gcm^{-3}$)	r_c (kpc)	J
NFW	6.44	0.383	26.3
NFWu	4.47	0.560	22.7
NFWd	10.90	0.228	30.6
Two-component model: inner NFW	1.11×10^4	5.5×10^{-3}	96
Two-component model: inner Moore	3.1×10^3	8.4×10^{-3}	124
Two-component model: outer NFW	0.81	1.32	
M 31			8.1

3.2 Mass models with two components

Case 1: The inner component is a CDM sub-halo The outer halo component is fitted by an NFW model with $\sim 1kpc$ scale, which is the value expected by making the model in Fig. 3 evolve from z = 4 to a present concentration parameter ~ 10. Then, the inner component is fitted with either a NFW profile (Fig. 5) or a Moore profile. The model parameters are given in Table 1. The integral of ρ^2 (J) is deduced from the density profile and the distance (the same integral for M31, calculated with the same interface, is also given for scaling).

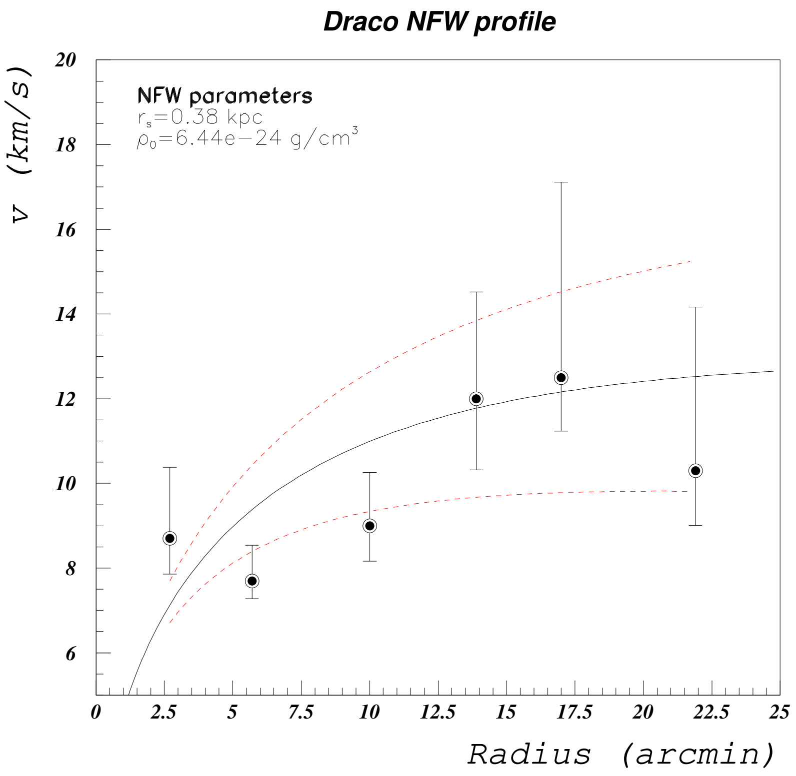

Fig. 4. Velocity model obtained by fitting an NFW density profile to the mean velocities. The NFW velocity curves indicated by dashed lines are fits to $v - 1\sigma$ (NFWd) and $v + 1\sigma$ (NFWu).

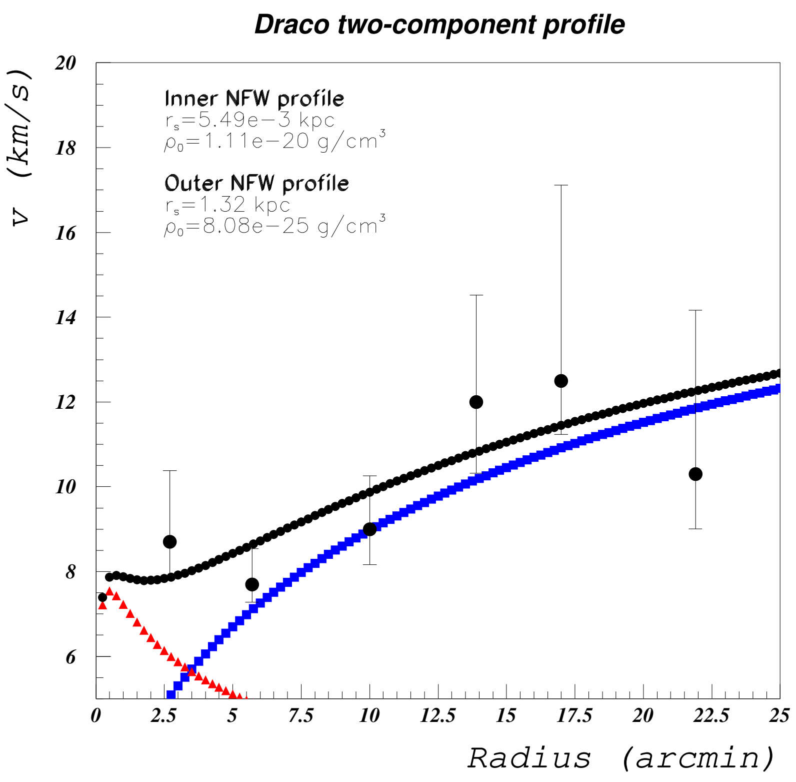

Fig. 5. Draco two-component mass model with inner and outer NFW profiles

Case 2: The inner component is a black hole with a spike of CDM The hypothesis of an inner compact CDM halo is plausible but, if taken at face value, the first velocity point alone indicates that there are $\sim 9 \times 10^5\ M_\odot$ within 60 *pc*, which is enormous. Another viable possibility is that the inner departure from the outer halo be due to a massive black hole (MBH). The CDM distribution around the black hole has been calculated in various scenarios. If the surrounding material is dense and has low velocity dispersion, the MBH makes a strong spike and increases adiabatically. This scenario, studied in [27], presumably occurred at the early stage of MBH formation. A number of criticisms were made on this scenario mainly on its ability to survive over Gigayears [28]. In particular, galaxy merging and MBH spinning in the galaxy potential will destroy the spike and dynamically heat the surrounding CDM gas. Nevertheless, in a stable environment the MBH will continuously reconstruct a spike in a short dynamical scale as we have numerically tested [29]. The best fit with a central MBH and an NFW outer halo with scale radius $r_s = 1.3\ kpc$ yields a central mass $M = 6 \times 10^5\ M_\odot$ (Fig. 6).

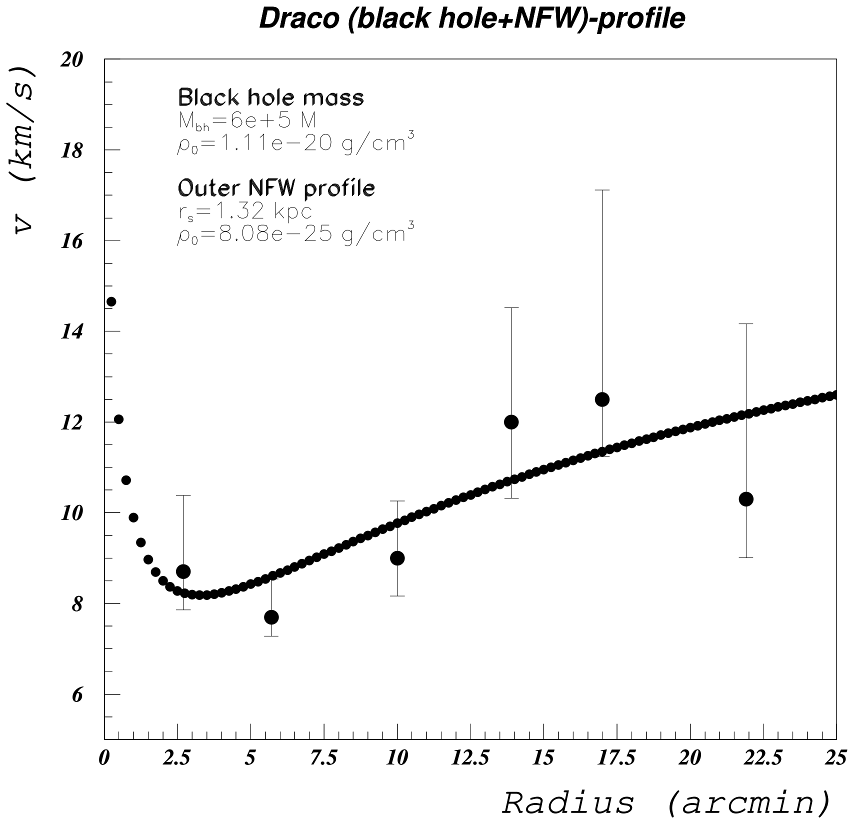

Fig. 6. Draco two-component mass model with a massive black hole and an outer NFW profile

Since we do not know what fractions of the central mass lie in the MBH and in the CDM spike, we consider a grid of models dominated by the MBH. We explore the mass and density parameter space by considering models where the CDM mass fraction is 0.1, 0.01, and 0.001 (with respect to the MBH mass) and is concentrated in an NFW sphere with scales $r_s = 0.1\ pc$, $0.34\ pc$, and $1\ pc$. The results in Table 2 clearly show that models with the highest masses and densities yield rather large values of J.

4 High energy γ-ray flux prediction for the benchmark models

4.1 The neutralino

Physics beyond the standard model could be supersymmetry. In constrained minimal supersymmetric extensions of the standard model, universality is assumed at some Great Unification Theory (GUT) scale for the gauge couplings, gaugino masses, soft-supersymmetry breaking scalar masses for squarks and sleptons, trilinear coupling and Higgs fields. If R-parity is conserved, the lightest supersymmetric

Table 2. Spike parameters for models with central MBH assuming $M_{MBH} = 6 \times 10^5\ M_\odot$

model	χ mass fraction	ρ_0 $(10^{-21}\ gcm^{-3})$	r_s (pc)	J
BH+NFW1	0.1	6.4×10^4	0.1	15529
BH+NFW2	0.01	6.4×10^3	0.1	173
BH+NFW3	0.001	6.4×10^2	0.1	20
BH+NFW4	0.1	2.1×10^3	0.34	665
BH+NFW5	0.01	2.1×10^2	0.34	24.8
BH+NFW6	0.001	21	0.34	18.4
BH+NFW7	0.1	1.11×10^2	1	65.9
BH+NFW8	0.01	11	1	18.8
BH+NFW9	0.001	1.1	1	18.3
M 31				8.1

particle, the so-called neutralino, is stable. The neutralino comes out as a combination of superpartners of neutral gauge bosons and Higgs bosons: it is a natural candidate for CDM. Being a Majorana particle, the neutralino is its own antiparticle which annihilates through various channels, several of them ending in high energy γ-rays.

4.2 From the GUT scale to the ElectroWeak (EW) scale with two programs

In order to derive present-day annihilations we use a code made of two parts: i) SUSPECT [23], which starts from the 5 mSUGRA free parameters (universal scalar mass, gaugino mass, trilinear coupling, tan β, sign(μ)) at the GUT scale and evolves the SUSY Lagrangian to the EW scale, and ii) DarkSUSY [24], which calculates masses, couplings and branching ratios at the EW scale from SUSPECT values. The code checks the conditions imposed by experimental measurements and by the relic density constraint $0.1 < \Omega_\chi h^2 < 0.3$, then derives the γ fluxes.

4.3 Benchmark models

The SUSY benchmark models have been proposed to provide a common way of comparing the discovery potential of future accelerators [25]. These scenarios correspond to 13 configurations of the 5 mSUGRA parameters with the trilinear coupling parameter A_0 set to 0. We calculate the γ fluxes expected from DRACO for the five benchmark models B,C,G,I,L with the same prescriptions as in [25] and for the "ground-level" model of M31 which will be used to recover the entire set of supersymmetric models by simple scaling (see below). The fluxes are given in Table 3. They are integrated above a threshold energy of $1 GeV$ and within an angle of $10^{-3}\ sr$. The "ground-level" model, calculated from the same procedure, corresponds to the astrophysical case where: 1) an average halo forM 31 is condidered, 2) a possible spike due to its central black hole is ignored, and 3) the clumpiness factor is also ignored. The flux units in Table 3 are $10^{-12}\ cm^{-2}s^{-1}$.

Table 3. Fluxes ($10^{-12}\ cm^{-2}s^{-1}$) at threshold energy 1 GeV for 5 benchmark models.

model	B	C	G	I	L
M31 NFW	0.97	0.095	0.55	3.44	2.6
DRACO NFW	3.06	0.30	1.73	10.8	8.3
DRACO inner NFW	11.6	1.14	6.6	41.3	31.2
DRACO inner Moore	15	1.47	8.5	53.3	40.3
DRACO BH+NFW1	1859	182	1054	6594	4984
DRACO BH+NFW2	20.7	2.0	11.8	73.6	55.6
DRACO BH+NFW4	79	7.79	45.1	282	213
DRACO BH+NFW7	7.8	0.77	4.5	28	21

5 Scaling DRACO with M31

Figure 7 shows the flux prediction above 30 GeV arising from the ground-level model of M 31, and the entire set of supersymmetric models within an angle of 1.4×10^{-4} sr. The fluxes for the five benchmark models calculated under the same conditions are identified around the "bulk region". The DRACO-to-M31 flux ratios are used to recover the entire neutralino space parameter for DRACO from that which was simulated in detail for M 31 [26].

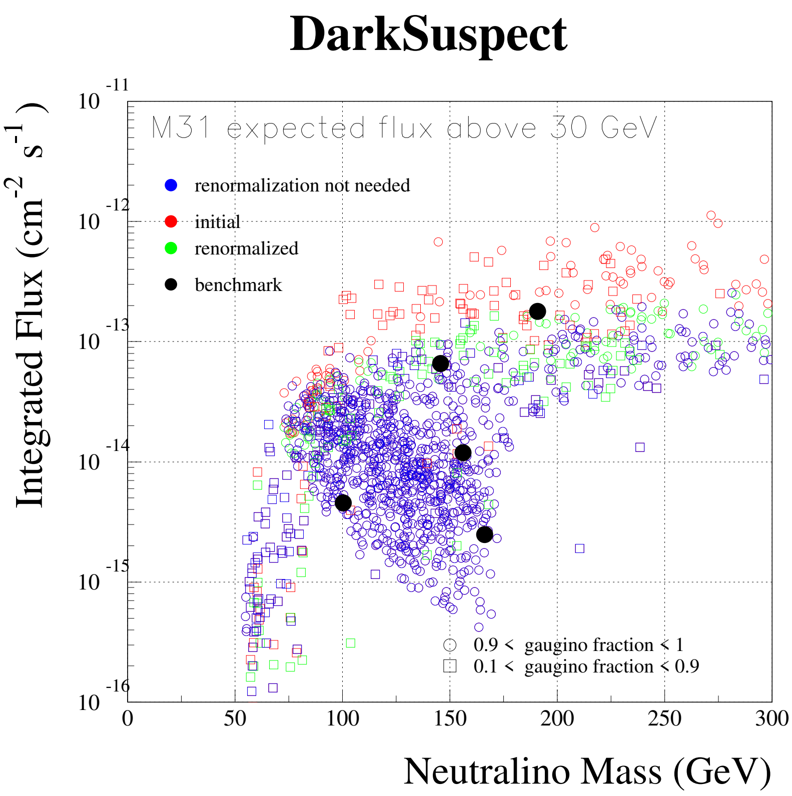

Fig. 7. High energy photon flux expected for M31 from simulations in [26]. The five benchmark models are identified. These fluxes have to be multiplied by a factor 12 (inner NFW profile) or 15 (inner Moore profile) to obtain the expected fluxes for DRACO and by another factor $O(1)$ for clumpiness.

Then the flux from the ground-level model of M 31 was convolved with CELESTE technical parameters in order to derive the number of γ expected with CELESTE. The DRACO fluxes were obtained by using again the DRACO-to-M31 flux ratios. For example to obtain the flux from DRACO, the fluxes fom "M 31 ground-level" must be multiplied by ~ 12 in the case of an inner NFW profile. If the central density of DRACO follows a Moore's profile in $r^{-1.5}$, a multiplicative factor of 15 should be used. The expected number of γ photons in 30 h ON-source has been calculated for the brightest neutralino models and the I benchmark model, for the various density distributions which we have considered. These numbers are given in Table 4.

Astrophysical models with an MBH surrounded by a very dense spike blow up the expected flux. At this point it is worthwhile reminding that all neutralino models have equal weight. Those producing the highest fluxes correspond to the largest annihilation cross-sections compatible with cosmology. Finally we have not taken into account the clumpiness factor which, in any case, is > 1 but should be $< O(10)$ in the inner region and $O(100)$ at large radii [30]. **In conclusion, there are models giving fluxes in the range $0.01 \times$ Crab and $1 \times$ Crab. Therefore, some fraction of the parameter space above the I benchmark model may be within CELESTE's reach under favourable astrophysical conditions.**

Table 4. Number of γ expected during 30h of CELESTE ON-source integration.

model	I	brightest	Comment
Inner NFW	11	76	no
Inner Moore	14	95	no
Inner Moore x 2 for clumps	27	**190**	maybe
BH+NFW1	1741	**11835**	yes
BH+NFW2	19	**130**	maybe
BH+NFW4	74	**503**	maybe

References

1. E.A. Baltz, C. Briot, P. Salati, R. Taillet, J. Silk 1999, astro-ph/9909112
2. J. Kleyna, M.I. Wilkinson, N.W. Evans, G. Gilmore 2001, astro-ph/0109450
3. M.I. Wilkinson, J. Kleyna, N.W. Evans, G. Gilmore 2001, astro-ph/0109451
4. J. Kleyna, M.I. Wilkinson, N.W. Evans, G. Gilmore 2001, astro-ph/0111329
5. E. Hayashi, J.F. Navarro, J.E. Taylor, J. Stadel, T. Quinn 2001, astro-ph/0203004
6. B. Moore, C. Calcáneo-Roldán, J. Stadel, T. Quinn, G. Lake, S. Ghigna, F. Governato 2001, astro-ph/0106271
7. M. Matteo 1998, ARAA 36, 435
8. X. Hernadez, G. Gilmore, D. Valls-Gabaud 2000, astro-ph/0001337
9. B. Moore 1994, Nature 370, 629
10. R.A. Flores, J.R. Primack 1994, ApJ 427, L1
11. J.R. Primack 2001, astro-ph/0112255
12. J.F Navarro, C.S. Frenk, S.D. White 1996, ApJ 462, 563
13. B. Moore, S. Ghigna, F. Governato, G. Lake, T. Quinn, J. Stadel, P. Tozzi 1999, ApJL 524, L19
14. S. Ghigna, B. Moore, F. Governato, G. Lake, T. Quinn, J. Stadel 1998, MNRAS 300, 146
15. A. Klypin, A.V. Kravstov, O. Valenzuela, F. Prada 1999, ApJ 522, 82
16. V. Springel, S.D. White, G. Tormen, G. Kauffmann 2001, MNRAS 328, 726
17. B. Moore, T. Quinn, F. Governato, J. Stadel, G. Lake 1999, MNRAS 310, 1147
18. P. Coté, S. G. Djorgovski, G. Meylan, S. Castro, J.K. McCarthy 2002, astro-ph/0203410
19. E. Giraud, G. Meylan, M. Sapinski, A. Falvard, A. Jacholkowska, K. Jedamzik, J. Lavalle, E. Nuss, G. Moultaka, F. Piron, P. Salati, R. Taillet 2002, to appear in ESO-ESA-CERN Conference, Garching 4-7 March 2002
20. D.J. Westpfahl, P.H. Coleman, J. Alexander, T. Tongue 1999, AJ 117, 868
21. E. Giraud 2000, ApJL 544, L41
22. C. Tyler 2002, astro-ph/0203242
23. http://www.lpm.univ-montp2.fr:7082/~ kneur/suspect.html
24. http://www.physto.se/~ edsjo/darksusy
25. J. Ellis, J.L. Feng, A. Ferstl, K.T. Matchev, K. Olive 2001, astro-ph/0110225
26. A. Falvard, E. Giraud, A. Jacholkowska, K. Jedamzik, J. Lavalle, E. Nuss, G. Moultaka, F. Piron, P. Salati, M. Sapinski, R. Taillet 2002, to appear in ESO-ESA-CERN Conference, Garching 4-7 March 2002
27. P. Gondolo, J. Silk 1999, astro-ph/9906391
28. D. Merritt et al. 2002, astro-ph/0201376
29. A. Dearaujo, E. Giraud "Simulations N-corps au voisinage du trou noir de M31" Note interne du GAM
30. C. Calcáneo-Roldán, B. Moore 2000, astro-ph/0010056